

Nice job (A)

APPLICATIONS OF HOLOGRAPHY: INTERFEROMETRY FOR MECHANICAL STRESS AND VIBRATION MEASUREMENT

Paul D. Friedberg
EE390F, Fall 2004

Abstract

Holographic interferometry can be used to characterize deformations of various structures under stress. In "double-exposure" holographic interferometry, two holograms of the same object, one of which is created while the object is under stress or some other form of excitation, are formed in the same photographic material. In "real-time" holographic interferometry, the superposition of a hologram of an object with the object itself (while being subjected to stress) is observed. In "time-average" holography, a hologram is created while the object in question is subjected to a source of periodic stress (such as vibration). These techniques are used to reveal the vibrational-response and stress-response characteristics of structures by examination of the fringe patterns in the resulting interferograms. Holographic interferometry is used for a wide array of exotic applications, such as mapping the vibrational response spectra of musical instruments and jet engine components, detecting buried mines, or examining the structural health of a priceless painting. Finally, digital holographic techniques have enabled the characterization of MEMS structures to assess the fabrication process (by examining residual stress) as well as the testing of MEMS's deformation responses to thermal loading.

I. INTRODUCTION

Before we examine applications of holographic interferometry, we must of course understand the principles behind holographic interferometry. To that end, we will briefly review holograph and interferometry, and then see how the two sciences are combined to create holographic interferometry. This section (as well as the second section, on the various types of holographic interferometry) closely follows the derivations contained in Vest's seminal holographic interferometry text [1].

I.A: Holography

Holography is a technique used to record and then later reconstruct the light field scattered by an object. The light wave scattered by the object in question is referred to as the object wave. To reconstruct the object wave, a second light wave, called the reference wave, is created such that it is coherent with the object wave. The two waves are directed onto the same photographic recording material, and the resulting recording of the interference pattern that arises is called a hologram. (A

common configuration of the holographic setup is shown in Fig. 1.) Expressing the recording step mathematically, we have the object wave, which can be expressed as

$$U_0(x, y) = a_0(x, y) \exp[-j\phi(x, y)], \quad (1)$$

the reference wave, which can be expressed as

$$U_R(x, y) = a_R, \quad (2)$$

and the resulting recorded intensity at the plane of the recording material:

$$\begin{aligned} I(x, y) &= |a_R + U_0(x, y)|^2 \\ &= a_R^2 + |U_0(x, y)|^2 + a_R U_0(x, y) + a_R U_0^*(x, y) \end{aligned} \quad (3)$$

The developed recording material will have a transmittance proportional to the recorded intensity:

$$t(x, y) = t_b + \beta(a_R U_0(x, y) + a_R U_0^*(x, y)) \quad (4)$$

where t_b will be nearly uniform over the film, therefore representing a bias level in the exposure. β is the sensitivity parameter of the recording material.

To reconstruct the object wave, the hologram is illuminated by a uniform wave (often simply the reference wave itself):

$$U_C(x, y) = a_C, \quad (5)$$

leading to the reconstructed wave:

$$\begin{aligned} U_R(x, y) &= U_C(x, y) * I(x, y) \\ &= a_C t_b + \beta a_C a_R U_0(x, y) + \beta a_C a_R U_0^*(x, y) \end{aligned} \quad (6)$$

The term $\beta a_C a_R U_0(x, y)$ is proportional to the object wave, assuming the $a_C a_R$ term is uniform. By filtering other components, we have reconstructed a facsimile of the object wave.

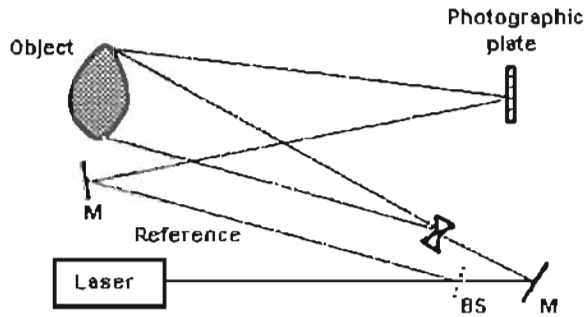


Figure 1. Common holographic setup. [12]

Holography is a significantly more thorough (and difficult) method of capturing the image of an object than simply measuring the intensity at a plane some distance from the object (e.g., via photography). In holography, since the object wave itself is reconstructed, not only the magnitude of the light scattered from the object but also the phase of that light is recorded. Thus, when viewed from slightly different angles, the holographic image will appear to have the same three-dimensional characteristics as the original object itself.

I.B: Conventional Interferometry

In conventional interferometry, an object wavefront is combined with a reference wavefront to create an interference pattern at the detector which allows for an understanding of the variations in the object wavefront. For example, interferometry is often used to create maps of the aberrations of an optical element, as in the case of the Micro-Exposure Tool (MET) optic at LBNL's EUVL laboratory. As shown in Fig. 2, light is bounced off the

MET optic, then split into two spherical waves. The first wave is created by passing the light through a relatively large window, allowing the aberrated wavefront of the optic to propagate; the second wave is the unaberrated reference wavefront, created by passing the light through an adjacent pinhole. The resulting interferogram of the unaberrated reference wave and aberrated optic wave enable accurate characterization of the optic.

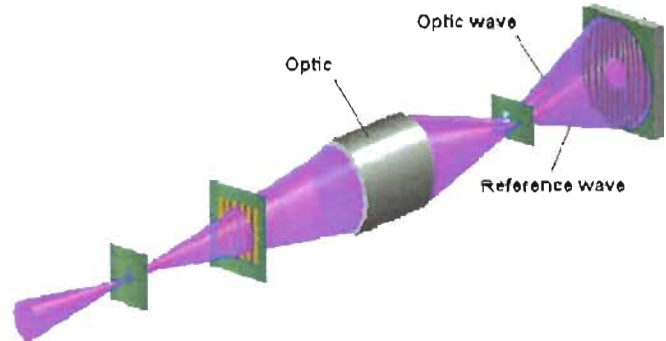


Figure 2. Setup for Interferometry of the MET optic. (Ken Goldberg, LBNL)

1.C: Holographic Interferometry

Combining conventional interferometry with holography, one can produce three-dimensional interferograms—images of diffusely-reflecting, three-dimensional objects that are overlaid with interference fringes indicating areas of deformation or displacement in the object. Similarly, transparent objects will be overlaid with fringes indicating a change in refractive index of the material as due to a structural deformity or change in thickness. Such interferometry is possible because the light field scattered from an object may be first holographically recorded, then later holographically reconstructed and compared to another light field scattered from the same object under different conditions, all with interferometric precision. This type of interferometry, called holographic interferometry, is defined as interferometry in which at least one of the waves in question is holographically reconstructed. The combination of two or more waves (of which one is a hologram) is referred to as a holographic interferogram (whereas a simple interference pattern recorded on a flat screen in intensity—as by the eye—is referred to simply as an interferogram, no modifier).

II. TYPES OF HOLOGRAPHIC INTERFEROMETRY

There are several flavors of holographic interferometry, but most rely on a similar basic principle: the combination of (1) a reference hologram recorded while the object is in neutral equilibrium, with no stress

applied, and (2) a second image or holographic image (which we'll refer to as the "subject image" or "subject hologram") created while the captured is being subjected to some form of stress—mechanical, thermal, vibrational, etc. In some cases, even a single hologram may be sufficient for the purposes of holographically interferometry. This section will review three basic types of holographic interferometry: double-exposure, real-time, and time-average holographic interferometry.

II.A: Double-exposure holographic interferometry

In double-exposure holographic interferometry, both the reference hologram and subject hologram are recorded in the same photographic plate. The exposures are made using a standard off-axis holographic imaging system as shown in Fig. 1. Upon development, the plate will then be illuminated using the reference beam, and the resulting hologram observed will consist of a three-dimensional image of the original object, overlaid with a pattern of interference fringes. Notably, the arrangement of the fringes will change as the viewing angle shifts, in similar fashion to the viewing of a single hologram.

To understand the origin of the fringes, we'll begin by writing down the two fields that are recreated using the double-exposure hologram. The first field—the field of the object captured in the reference hologram—is written as:

$$U_0(x, y) = a(x, y) \exp[-j\phi(x, y)] \quad (7)$$

The second field—the field of the stressed object captured in the subject hologram—is affected primarily by a phase change due to the deformation:

$$U_0'(x, y) = a(x, y) \exp[-j\{\phi(x, y) + \Delta\phi(x, y)\}] \quad (8)$$

The observed intensity of the reconstructed wave is given by:

$$\begin{aligned} I(x, y) &= |U_0(x, y) + U_0'(x, y)|^2 \\ &= |a(x, y) \exp[-j\phi(x, y)] + \\ &\quad a(x, y) \exp[-j\{\phi(x, y) + \Delta\phi(x, y)\}]|^2 \\ &= 2a^2(x, y) \{1 + \cos[\Delta\phi(x, y)]\} \end{aligned} \quad (9)$$

The fact that the fields (and not intensities) of the two object waves add is the crux of holographic interferometry—it is what makes interferometry by holography superior to classical interferometry, particularly when investigating three dimensional effects.

It is the linearity of the holographic process that gives rise to this phenomenon of field addition.

As Eq. 9 shows, the observed intensity will consist of the intensity of the original object modulated by the fringe pattern $\{1 + \cos[\Delta\phi(x, y)]\}$. Dark fringes indicate positions where the subject hologram and reference hologram are perfectly out of phase (that is, $\Delta\phi$ is an odd-integer multiple of π), and light fringes are positions where the subject and reference holograms constructively interfere ($\Delta\phi$ is an even-integer multiple of π). Moving from one fringe to another corresponds to an out-of-plane displacement of the object that is equal to half the wavelength of the illuminating light. The location and density of these fringes may therefore easily be related to physical qualities of the object under study.

II.B: Real-time holographic interferometry

In some cases, it is necessary or useful to observe the response of the object under study to changing excitation in real time. In particular, when mechanical vibrations are the subject of concern—for example, if one wants to identify the resonant frequencies of a given object by sweeping the excitation frequency over a wide range of values—"real-time" holographic interferometry is the best choice. In real-time holographic interferometry, the light scattered by the object interferes by superposition with the holographically reconstructed image of the object itself, recreated using a reference hologram taken under at-rest conditions. The configuration used for real-time holographic interferometry is identical to that used for double-exposure holographic interferometry. The reference hologram is recorded, developed, and returned to the recording plane. When the laser is turned back on, the hologram will be illuminated simultaneously by the reference wave and the light scattered by the object under some kind of varying excitation. The observer will then see the interference of the two waves (holographic and object) that will describe not only the deformity or displacement of the object but that will also indicate vibrational amplitude of the excitation.

Mathematically, if the complex amplitude of the holographically reconstructed wave is $U_0(x, y)$, then the instantaneous object wave can be expressed as $U_0(x, y) \exp[j\Delta\phi(x, y, t)]$, where $\Delta\phi(x, y, t)$ is the phase change due to the vibration at time t . The instantaneous intensity observed during real-time holographic interferometry will then be:

$$\begin{aligned} I(x, y, t) &= |U_0(x, y)|^2 * |1 + \exp[j\Delta\phi(x, y, t)]|^2 \\ &= |U_0(x, y)|^2 * 2\{1 - \cos[\Delta\phi(x, y, t)]\} \end{aligned} \quad (10)$$

In real-time holographic interferometry, the fringes arise from the $\{1 - \cos[\Delta\phi(x, y, t)]\}$ term in Eq. 10.

To constitute real-time holographic interferometry, the image must be recorded in real-time by a CCD sampling at a rate exceeding the vibration frequency. Another option would be to use a stroboscopic technique, whereby the laser is strobed at the vibrational frequency. Then a snapshot of the object at a single point (or more likely, a very short window) during the vibrational cycle can be recorded; to take a snapshot at a different point in the cycle, the laser should simply be phase-delayed by the desired fraction of the total vibrational period.

If, instead, the image is photographed with a shutter speed longer than the vibrational period, or is viewed by the eye (which is limited to viewing frequencies of about 25 Hz), and then the time-averaged intensity is recorded. This would result in an observed fringe pattern, but one with significantly less fringe visibility than can be accomplished using a simpler time-averaging technique visited in the next section.

II.C: Time-average holographic interferometry

In time-average holographic interferometry, a single holographic exposure is made during vibrational excitation. Naturally, the exposure period will be much longer than the vibrational period, thus a time-average view of the object field is recorded. Since an object under vibration spends most of its time near the positions of maximum positive or negative displacement (where it has zero velocity), the resulting hologram is qualitatively similar to a double-exposure interferogram, with the difference that it also displays contours of the object during the intermediate displacements between the two maxima.

As an example, consider an object vibrating sinusoidally:

$$z(x, y, t) = Z(x, y) \sin(\omega t) \quad (11)$$

Light reflected from a given point on the object is phase delayed by:

$$\Delta\phi(x, y, t) = (2\pi / \lambda) * 2Z(x, y) \sin(\omega t) \quad (12)$$

Therefore, the sum of the object and reference waves will have the form:

$$U_0(x, y, t) = a(x, y) \exp[-j\{\phi(x, y) + \frac{4\pi}{\lambda} Z(x) \sin \omega t\}] \quad (13)$$

Thus, when the time-average hologram is recorded and illuminated by the reference wave, the reconstructed wave

$U_R(x, y)$ will be proportional to the time-average of the object wave over the exposure interval T :

$$a(x, y) \exp[-j\{\phi(x, y)\}] * \frac{1}{T} \int_0^T \exp[\frac{4\pi}{\lambda} Z(x) \sin \omega t] dt \quad (14)$$

Since the exposure time is long compared to the vibrational period, $T \gg 1/\omega$, the integral evaluates to

$$U_R(x, y) = a(x, y) \exp[-j\{\phi(x, y)\}] * J_0\left[\frac{4\pi}{\lambda} Z(x)\right] \quad (15)$$

and the observed intensity will be:

$$I_R(x, y) = a^2(x, y) * J_0^2\left[\frac{4\pi}{\lambda} Z(x)\right]. \quad (16)$$

Thus, interference fringes will appear superimposed on the surface of the object, with bright fringes coinciding with (a) nodal regions of the object, where the object remains stationary during the vibration, and (b) regions of the object that experience constant vibrational amplitude. Based on these interference fringes, the vibrational amplitude of the object at any point can be extracted.

II.D: Practical concerns

In order to achieve successful use of holographic interferometry, extreme care must be taken to reposition the reference hologram (in the case of real-time or time-average interferometry) and perform development of the reference hologram so as to prevent any magnification or demagnification of the reconstructed image by swelling or shrinking of the recording material. In double-exposure holographic interferometry, there are fewer sources of mechanical error, although one must take care not to displace the object other than by the intended source of stress to prevent extraneous fringing effects in the resulting interferogram. These effects are an entire science alone, but for the scope of this paper they will not be examined in great detail.

III. APPLICATIONS OF HOLOGRAPHIC INTERFEROMETRY

Holographic interferometry has many uses, several of which will be presented here. The major thrust of this overview will consider uses of holographic interferometry in nondestructive testing (NDT). In nondestructive testing, holographic interferometry is used to characterize deformations of various structures under stress. NDT techniques via holographic interferometry are used to

measure vibration and stress-response characteristics of structures including jet engines [2] and musical instruments [5]. In addition, digital holographic techniques [7,8] have enabled the characterization of MEMS structures to assess the fabrication process (by examining residual stress) as well as the testing of MEMS's deformation responses to thermal loading, etc [5,6]. Finally, holographic interferometry is used for more exotic applications, such as detecting buried, non-metallic antipersonnel mines [3] and evaluating the structural integrity of aging priceless works of art [4]. We will visit each of these examples in detail.

A. Dynamic vibration analysis of a jet turbine compressor rotor [2]

An aircraft engine is an excellent example of a mechanical component that requires developmental engineering for high-stress applications. To guarantee the engine can tolerate extremes in vibration as well as impulsive or continuous stress, the vibrational modes, common displacements and motion geometries of the part must be understood. To that end, holographic interferometry has been employed to provide real-time, nondestructive metrology that not only identifies the characteristics of normal operation of a jet turbine compressor (Figs. 3-4) but also to search for hidden structural weaknesses or other anomalies/defects which would compromise the integrity of the component.



Figure 3. Turbine compressor, front view. [2]



Figure 4. Turbine compressor, back view. [2]

The techniques used for this study encompassed both real-time and time-average holographic interferometry. First, using a standard holographic setup, a holographic exposure of the turbine structure was made in a stress-free state. This initial holographic image was then left in place, the structure was excited by a low-level non-contact acoustical source, and the real-time holographic image containing the superposition of the stress-free hologram and excited turbine was collected by a camera. The vibrational frequency was then swept across the range of interest and particularly strong resonances were noted.

Then, using time-average holographic techniques, interferograms of the strong resonances were recorded, and based on interference fringes produced by the vibrational stresses, mappings of the displacement responses of the part could be acquired. Figs. 5-6 show samples of interferograms of both the front and back, respectively, of the turbine. The complex shapes of the interference patterns demonstrate the strong nodal behavior of the part, with nodal "ridges" that divide the high-amplitude fringe groups indicating a phase change the occurs between them. These pictures also illustrate and define high-stress points in the part that might be especially susceptible to manufacturing defects.

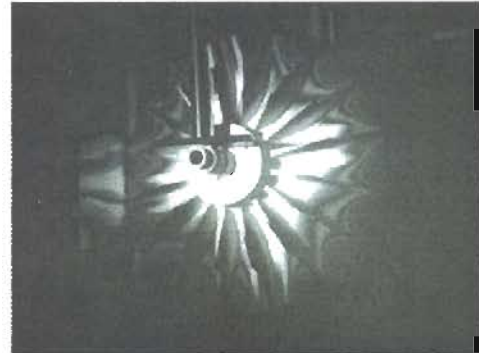


Figure 5. Holographic interferogram of a turbine compressor, front view. [2]

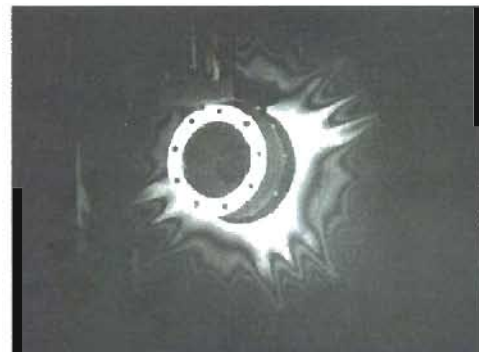


Figure 6. Holographic interferogram of a turbine compressor, back view. [2]

In addition, the strongest resonant modes of the part can be identified. Some particularly strong resonant modes are displayed in Fig. 7. This information provides critical clues to engineers about the susceptibility of the part to failure due to excitation at those resonant frequencies.

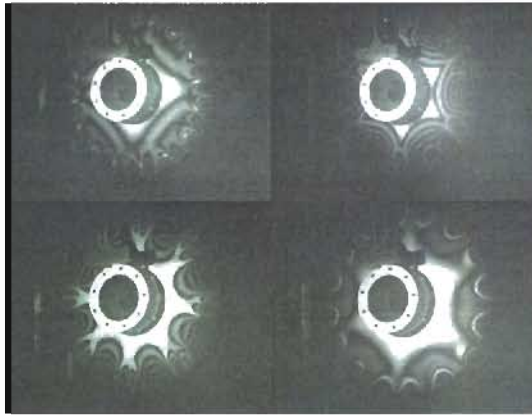


Figure 7. Holographic interferograms of a turbine compressor, for various strong resonances. [2]

B. Non-metallic antipersonnel mine detection [3]

A number of techniques are used to detect buried mines. Most are based on magnetic, radar, or chemical detection schemes. However, several types of mines contain very few metallic parts, and as such are difficult to detect with traditional techniques. Although seismic detection techniques have been used for marine mines, they have not been previously adapted to buried mines; however, by combining seismic detection techniques with holographic interferometry, perturbations in the propagation of a seismic wave caused by a buried mine can be observed.

The technique employs holographic interferometry in a similar configuration used to detect defects in mechanical structures. For demonstration's purposes, a mine was buried in a sandbox. A pulsed laser is used to make two holograms of a target area of the surface of the sand box at two very close times (Fig. 8).

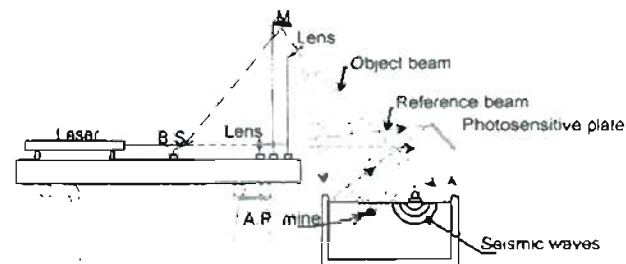


Figure 8. Experimental setup for proof-of-concept of holographic mine detection. [3]

The first holographic exposure is made with no excitation of the sand box. The second exposure is made after triggering a seismic wave. The propagation of the seismic wave creates slight, periodic displacements on the surface of the sand box, appearing as a series of radially expanding interference fringes when the two holographic images are combined. The presence of a deviation in density of the contents of the sand box will make a clear deformation in this radial pattern as shown in Fig. 9, signaling the presence of the mine.

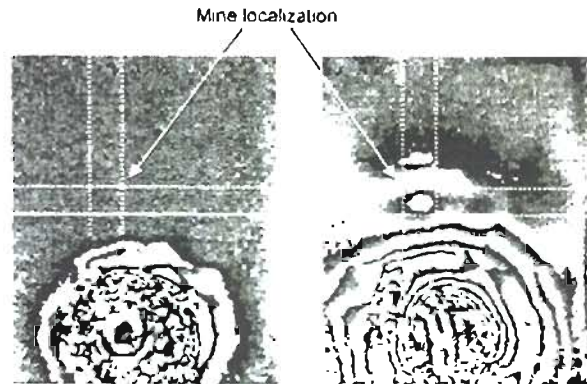


Figure 9. Mine detection illustration; the deviation in the expanding fringe pattern of the seismic wave indicates the mine position. [3]

C. Painting diagnostics [4]

Over time, priceless paintings suffer damage due to humidity, temperature variations, and other unavoidable, everyday occurrences. More specifically, paintings are structurally composed of several layers of primers, made of mixtures of gesso and glue, and paint, all stacked upon a canvas or wood base. As a result of slowly-accruing damage to a painting, detachments between layers can occur, usually between the first layer of primer and the wood (or canvas) base. These detachments, of course, are harmful to the health of the painting, and need to be monitored to allow for identification of works which require restoration.

Double-exposure holographic interferometry is a proven method for measuring the location and severity of the detachments. Due to natural temperature and humidity variations, it is found that local displacements in detachments occur at a rate on the order of a few microns per minute. Therefore, by recording each of the exposures in the double-exposure holographic interferometry setup with a separation of several minutes, fringe patterns on the surface of the painting will be sufficiently dense to identify detachments. However, to heighten the sensitivity of the method, slightly warmed air

is passed over the surface layers of the painting; since the detached regions of the painting will disperse heat into the canvas or wood support more slowly than “healthy” parts of the painting, these regions will stand out with higher contrast (more fringes) in a holographic interferogram recorded during the cooling phase. As shown in Fig. 11, the detachments appear as dislocations in the fringe pattern of the cooling painting.



Figure 10. Holographic image of a panel painting (*Santa Caterina*, Pier Francesco Fiorentino, fifteenth century). [4]



Figure 11. Holographic interferogram made using thermal-drift method, revealing detachments. [4]

D. Deflection shapes of the violin body [5]

Even today, the fundamental physical function of the violin is not well understood. Since the late 1960's, however, holographic interferometry has been a critical tool in extracting some basic information about the instrument's strong resonance and responses to different bowed stimuli on the strings. In particular, the vibration modes of both the top-plate and bottom-plate of the instrument have been identified.

To accomplish this mode-mapping task, a phase-stepped version of real-time holographic interferometry with digital capture was employed. The violin was illuminated by laser light, creating an object wave incident on a CCD detector which was then interfered with a smooth reference beam. As shown in Fig. 12, a piezoelectric mounted mirror (PZM1) is used to create shifts in the optical phase of the object wave in steps of 90° . By overlaying the most recent 4 frames, a real-time interferogram is created that displays a maximum number of fringes when a strong resonance is found during a sweep of the excitation frequency. Some samples of holographic interferograms recorded at resonant frequencies are shown in Fig. 13.

The mapping of a violin's resonant frequency spectrum is frequently used as a first-order ranking system in the instrument's sound quality. Specifically, when particular resonant frequencies of a violin fall close to “principal peaks” of the violin, which are related to an acoustic phenomenon of bowed-string instruments called the wolf-tone phenomenon, the sound quality of the instrument is generally considered superior.

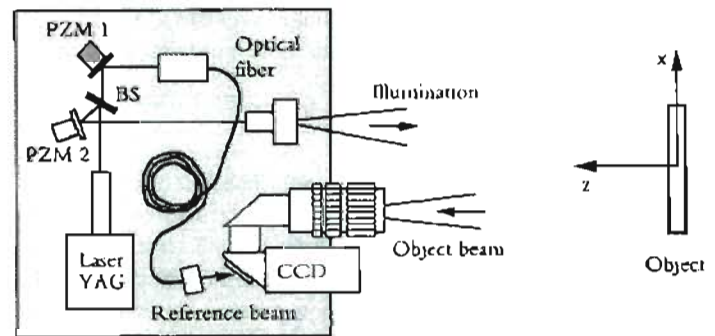


Figure 12. Set up for phase-stepped real-time holographic interferometry of a violin. [5]

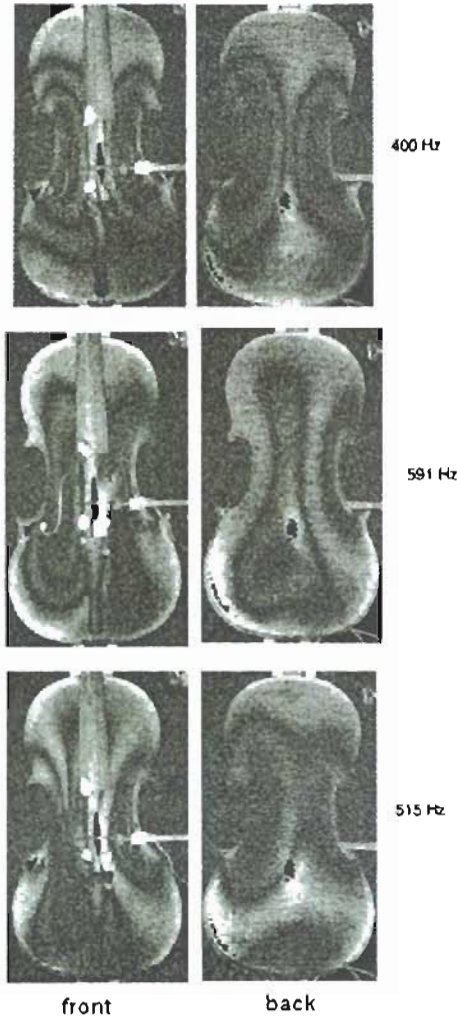


Figure 13. Holographic interferograms of some strong resonant frequencies of the violin. [5]

E. MEMS characterization [6,7]

Holographic interferometry has recently been used to perform measurements of MEMS structures. By accurate determination of the shape of a MEMS structure such as a cantilever beam following fabrication, one can evaluate the quality of the fabrication process by determining the residual stress in the MEMS structural layer, or evaluate the combination of different materials in the composition of the structures [6]. In addition, one can characterize the mechanical properties of the resulting structures under source of outside, operational stress, such as temperature gradients [7].

To expose a hologram of a MEMS structure, a digital holographic technique is used. As shown in Fig. 14, a laser illuminates the MEMS structure and the resulting object wave is combined with the reference wave (created using a beam splitter) at a CCD detector. This setup

requires the use of a microscope objective to enlarge the image of the object.

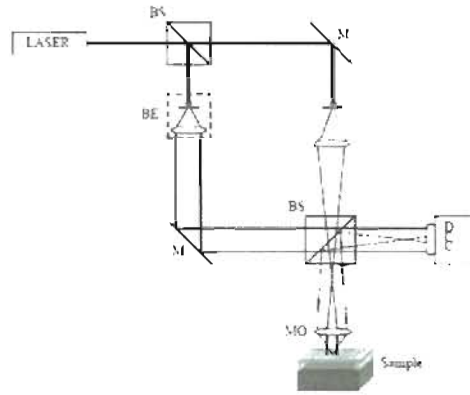


Figure 14. System for digital holographic interferometry of MEMS structures. [6]

Using a double-exposure holographic interferometry technique, one hologram is made of the cantilever under observation, and a second is made of the surrounding flat reference surface in close proximity to the cantilever. Since a digital holographic technique is used, the holograms are recorded separately and combined using DH techniques [8,9]. Using this technique, the resulting interferogram will be subject to some local errors due to local imperfections in the reference surface. However, assuming an acceptable reference surface, interference fringes are clearly visible on the interferogram and can be used to create an out-of-plane deformation map, as shown in Fig. 15.

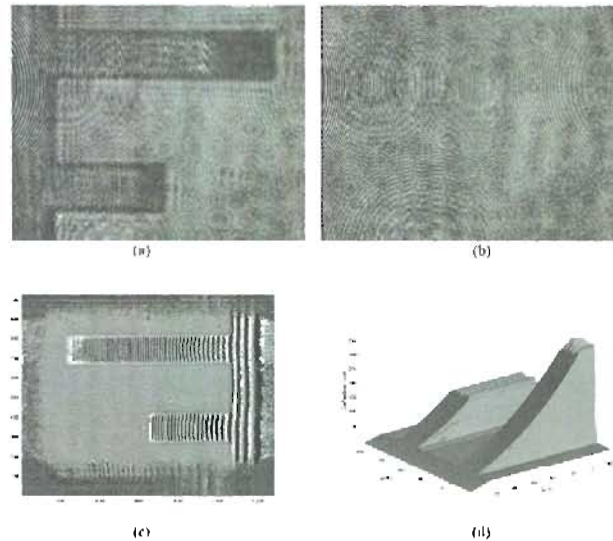


Figure 15. Holographic interferometry of a cantilever beam. (a) object hologram; (b) reference hologram; (c) composite DH double-exposure interferogram; (d) out-of-plane deformation map created using Interferogram [6]

As shown in Fig. 16, digital holographic interferometry can be used as a fast substitute for high-angle SEM photography in characterization of MEMS structures. Here, the interferogram clearly captures the complex warping of the cantilevers quite well.

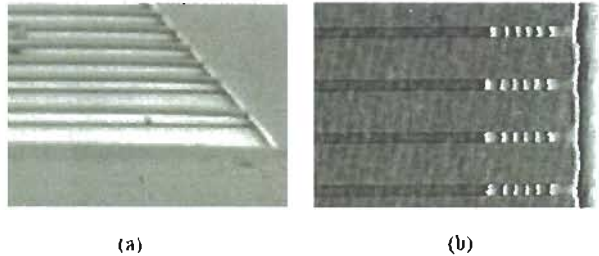


Figure 16. Comparison of SEM image and holographic interferogram of cantilever structures. (a) SEM image; (b) holographic Interferogram [7]

IV. SUMMARY

Holographic interferometry is technique used widely for characterizing the mechanical response of structures to sources of deformation. Through double-exposure holographic interferometry, one can detect flaws in a structure while under constant stress. With real-time holographic interferometry, one can perform a rapid sweep of vibrational excitation and look for resonant frequencies. Finally, using time-average holographic interferometry, one can create high-visibility interferograms of an object under vibrational stress for detailed study.

REFERENCES

- [1] Vest, C. M., *Holographic Interferometry*, Wiley, New York, 1979.
- [2] H. Fein, "An application of holographic interferometry for dynamic vibration analysis of a jet engine turbine compressor rotor," *Practical Holography XVII and Holographic Materials IX*, SPIE Vol. 5005, pp. 307-315, 2003.
- [3] F. Christnacher, P. Smigielski, A. Matwyschuk, M. Bastide, D. Fusco, "Mine detection by holography," SPIE Vol. 3745, pp. 361-365, 1999.
- [4] S. Amadesi, F. Gori, R. Grella, G. Guattari, "Holographic methods for painting diagnostics," *Appl. Opt.* 13, pp. 2009-2013, 1974.
- [5] A. Runnemalm, N. Molin, "On operating deflection shapes of the violin body including in-plane motions," *J. Acoust. Soc. Am.* 106, pp. 3452-3459, 2000.
- [6] G. Coppola, S. De Nicola, P. Ferraro, A. Finizio, S. Grilli, M. Iodice, C. Magro, G. Pierattini, "Characterization of MEMS structures by microscopic digital holography," *MEMS/MOEMS: Advances in Photonic Communications, Sensing, Metrology, Packaging and Assembly*, SPIE Vol. 4945, pp. 71-78, 2003.
- [7] P. Ferraro, S. De Nicola, G. Coppola, A. Finizio, M. Iodice, C. Magro, G. Pierattini, "Testing silicon MEMS structures subjected to thermal loading by digital holography," *Reliability, Testing, and Characterization of MEMS/MOEMS III*, SPIE Vol. 5343, pp. 235-243, 2004.
- [8] U. Schanrs and W. Juptner, "Direct recording of holograms by a CCD target and numerical reconstruction," *Appl. Opt.* 33, pp. 179-181, 1994.
- [9] U. Schanrs, "Direct phase determination in holographic interferometry using digitally recorded holograms," *J. Opt. Soc. Am. A* 11, pp. 2011-2015, 1994.
- [10] V. Ginzburg, "Some practical applications of holography in science and industry," *Practical Holography XII*, SPIE Vol. 3293, pp. 205-216, 1998.
- [11] G. Brown, "Thirty Odd Years of Industrial Hologram Interferometry," *International Conference on Applied Optical Metrology*, SPIE Vol. 3407, pp. 236-247, 1998.
- [12] H. Tiziani, G. Pedrini, "Digital holographic interferometry for shape and vibration analysis," *International Conference on Experimental Mechanics: Advances and Applications*, SPIE Vol. 2921, pp. 282-287, 1997.